Desalination and Water Treatment
www.deswater.com

doi: 10.1080/19443994.2015.1030123

57 (2016) 1388–1398
January

Taylor & Francis
Taylor & Francis Group

Role of micro-organisms present in diesel fuel in the microbiological corrosion of carbon steel St3S

Tomasz Słomczyński*, Maria Łebkowska

Faculty of Environmental Engineering, Department of Biology, Warsaw University of Technology, Nowowiejska 20, 00-653 Warsaw, Poland, Tel. +48 22 2347686, +48 22 6212979; email: tomasz.slomczynski@is.pw.edu.pl (T. Słomczyński)

Received 30 June 2014; Accepted 6 February 2015

ABSTRACT

This study presents the microbiological and chemical characteristics of the water taken from diesel fuel storage tanks. The growth of micro-organisms was monitored in accordance with the ASTM standard test. The observations of damage to St3S steel were made using a scanning microscope, and the composition of the formed corrosion products was determined using an energy dispersive spectroscopy analyser. Micro-organisms causing microbiological corrosion (sulphate-reducing bacteria, iron bacteria, fungi) were found to develop in the water and on the steel discs. The growth of micro-organisms was the most intense on the discs placed at the water–fuel interphase. Microscopic studies revealed that the disc fragment exposed to the organic phase (fuel) practically did not undergo any corrosion. In the water phase, corrosion was uniform, and its intensity increased with the proximity to the interphase. The highest degree of corrosion was observed on the surface of the steel in the area in which the water was in contact with the fuel. In this area, discs were subject to strong corrosion and formation of rather deep corrosion pits was observed. Gravimetric studies revealed that the corrosion weight calculated in V_m and V_p units is much higher at the water–fuel interphase than in the aqueous phase.

Keywords: Microbial corrosion; Biofilm; Carbon steel St3S; Scanning microscope; EDS

1. Introduction

Tanks that store fuels as well as oil and gas pipelines contain micro-organisms—bacteria and fungi that worsen the quality of fuels and cause corrosion. The number of micro-organisms in fuels is small, usually smaller than 50 CFU/L but can reach significant numbers, in exceeding of 10^6 CFU/ml, in the water layer that forms under the fuel. Numerous micro-organisms were observed in the fuel–water interphase. In diesel fuel storage tanks, bacteria of the genera *Acinetobacter*, *Aeromonas*, *Bacillus*, *Pseudomonas*, *Sphingomonas*, *Nocardia*, *Leptothrix* and *Siderocapsa,* as well as sulphate-reducing bacteria (SRB) are detected. Fungi are represented by the genera *Alternaria*, *Aspergillus*, *Fusarium*, *Penicillium*, *Rhodotorula*, *Trichoderma* and *Candida*. Similar groups of micro-organisms occur in containers with z gasoline, heating oil and kerosene. The corrosion is caused by micro-organisms that reduce

*Corresponding author.

Presented at the 12th Scientific Conference on Microcontaminants in Human Environment 25–27 September 2014, Czestochowa, Poland

sulphates, oxidize or reduce iron and manganese, and produce acids [1–4]. Corrosion studies embrace determination of metal loss, the content and diversity of micro-organisms as well as observations of structural and qualitative changes in the corroding surfaces [5]. In current microbiological studies, molecular methods enabling accurate identification of micro-organisms are more and more frequently used [6–9]. The prevailing methods for determining changes on the surface of metals include scanning electron microscope (SEM) combined with energy dispersive spectroscopy (EDS) and X-ray diffraction (XRD). These methods allow one to identify corrosion products [8–11]. Microbiological corrosion, which boils down to electrochemical corrosion, results in damage not only to steel and aluminium but also to many alloys and ceramic cover as wells.

The objective of the study was to determine the course of the microbiological corrosion of St3S construction steel in the environment of a diesel fuel storage tank.

2. Materials and methods

2.1. Samples

The samples consisted of water collected from drainage from a diesel fuel storage tank. In accordance with the standard test described in the Annual Book of ASTM Standard [12], the samples were introduced into 500 ml separators in which two layers formed: an upper fuel layer being about 5 cm high and the lower aqueous one. one-millimetre-thick St3S steel discs with the diameter of 20 mm were placed in the aqueous layer and in the oil–water interphase. The chemical composition of the steel in weight per cent was C-0.18, Si-0.3, Mn-0.5, P-0.045, S-0.05 and Cu-0.01. The discs were first sanded with grade 800 sandpaper and degreased with acetone. The roughness of the surface of the discs was R_a = 0.34 μm. The experiments were carried out at 22℃ in a thermostat under static conditions.

2.2. Chemical determinations

Determinations involved the aqueous layer in which pH, chemical oxygen demand (COD), the content of nitrogen compounds, phosphates and ether extract were assayed according to Polish Standards and ISO Standards.

2.3. Microbiological determinations

The total number of bacteria was determined on nutrient agar medium (MPA), 26℃, 72 h; most probable number (MPN) of iron bacteria belonging to the genus *Leptothrix*—on a medium containing birch leaf extract, 26℃, 14 d; MPN of iron bacteria belonging to the genus *Siderocapsa*—on medium with iron ammonium citrate, 26℃, 14 d; MPN of SRB on Starkey medium, 26℃, 7 d; and number of fungi on Martin medium 26℃, 7 d. Plating was carried out from the aqueous phase, from the fuel–water interphase as well as from the biofilm developing on the discs.

2.4. Identification of micro-organisms

The identification of bacteria was based on the morphological, cultural and biochemical traits of micro-organisms taken from grown colonies. To determine biochemical traits, API 20E, API20NE and API STAPH tests were used. The microbiological study was carried out in the aqueous phase and the water–fuel interphase.

2.5. Weight of corrosion studies

The weight of corrosion was determined on the basis of the loss of weight of washed discs, which were dried at 105℃ and weighed with accuracy 0.0001 g. The weight of corrosion in V_m (g/m^2 d) and V_p (mm/y) units was calculated from losses of mass according to the norm PN-78/H-04608. The studies involved discs placed in the aqueous phase and in the water–fuel interphase.

2.6. Microscope studies on the surface of the discs

Changes on the surface of discs from the water–fuel interphase were observed under on scanning microscope (Hitachi S-3500-N) equipped with the EDS spectrometer (Norman Ventage). EDS measurements allowed one to evaluate changes in the chemical composition of the surface of the discs.

2.7. Frequency of the studies

Chemical and microbiological determinations were carried out on 0, 7, 14, 21, 28, 35 and on day 42 of the experiment. Gravimetric studies of the discs exposed in the aqueous phase were conducted as above and after 56 d, whereas from the interphase after 7, 14, 21, 28, 35 and 42 d. Microscopic observations were conducted at the same intervals up to day 47 of the studies.

3. Results and discussion

3.1. Chemical studies

The chemical determinations of the water conducted over a period of 42 d revealed the some fluctuation of most indices. The water was characterized by high COD values from about 8,000 to over 15,000 mg O_2/L. An increase in the total nitrogen and ammonium nitrogen was observed in the course of the studies, which after 42 d reached 496.2 mg/L and 494 mg/L, respectively (Table 1).

3.2. Microbiological determination

The number of micro-organisms in the aqueous layer after the initial growth decreased except for iron bacteria belonging to the genus *Leptothrix and Siderocapsa* (Table 2). In the fuel–water interphase, an increase in the number of bacteria was observed, including the species *Sphingobacterium multivorum* and iron bacteria; after an initial drop, numerous SRB were identified (Table 3). Unlike the changes in the number of micro-organisms in the above-mentioned layers, some considerable growth of all groups of micro-organisms on the steel discs placed in the water and in the interphase was observed, reaching its maximum on days 35–42 of the study. A greater increase in the number of micro-organisms was observed in the case of the discs placed in the fuel–water interphase than in those from the water phase (Tables 4 and 5). The number of bacteria on the discs placed at the interphase reached 5.72×10^6 CFU/cm^2, the number of fungi 218×10^5 CFU/cm^2 and that of SRB $2{,}400 \times 10^3$ as MPN/100 cm^2. Iron bacteria belonging to the genus *Siderocapsa*—240×10^5 (MPN/100 cm^2) were also numerous.

3.3. Gravimetric studies

The weight of corrosion was much higher on the discs from the interphase than on those from the water layer, namely V_m to 2.14 g/cm^2 d, V_p to 0.099 mm/y and V_m to 0.32 g/m^2 d, V_p to 0.014 mm/y, respectively (Tables 6 and 7).

3.4. Scanning microscopic observations

Microscopic observations revealed that the discs placed in the water showed uniform corrosion whereas in the fuel–water interphase they were strongly corroded—the surface of the discs was characterized by pits whose depth increased with time from 54 to 130 μm (after 47 d).

The scanning microscope image of the surface of St3S carbon steel exposed for 7 d at the water–fuel interphase is shown in Fig. 1.

The chemical composition of corrosion products studied using EDS spectrometer is given in Figs. 2 and 3.

The analysis of the chemical composition of corrosion products after 7 d of exposure showed that at the interphase, they consisted mainly of iron oxides and hydroxides with small addition of silica and chlorine compounds (Fig. 2). However, below the interphase, the extent of corrosion was much smaller, with iron as the main compound found in the analysed area (Fig. 3).

The scanning image of the surface of St3S carbon steel samples exposed for 47 d at the water–fuel interphase is presented in Fig. 4.

The results of studies on the chemical composition of the formed corrosion products using the EDS spectrometer are given in Figs. 5–7.

Table 1
Results of chemical analysis of water

Parameter	Duration of the studies (d)						
	0	7	14	21	28	35	42
COD (mg O_2/L)	15,530	8,260	13,900	9,800	12,400	13,600	14,100
Ether extract (mg/L)	282	242	88	118	132	158	180
Total nitrogen (mg $N_{tot.}$/L)	361.7	369.4	367.5	399.5	461.3	487.7	496.2
Ammonium nitrogen (mg N-NH_4/L)	360	367	365	396	459	485	494
Organic nitrogen (mg N_{org}/L)	nd	nd	nd	nd	nd	nd	nd
Nitrite nitrogen (mg N-NO_2/L)	0.60	0.30	0.30	0.35	0.15	0.20	0.08
Nitrate nitrogen (mg N-NO_3/L)	1.1	2.1	2.2	3.2	2.2	2.5	2.1
Phosphates (mg PO_4/L)	20	18	15	17	21	23	18
Reaction	6.41	6.42	6.55	6.61	6.44	6.44	6.4

Note: nd—not determined.

Table 2
Number of bacteria and fungi in the water

Parameter	Duration of the studies (d)						
	0	7	14	21	28	35	42
Total number of bacteria, including	2.58×10^6	5.13×10^6	1.68×10^6	3.15×10^6	2.46×10^6	0.51×10^6	0.15×10^6
Flavobacterium indologenes (CFU/ml)	2.42×10^6	0.13×10^6	nd	nd	nd	nd	nd
Sphingobacterium multivorum (CFU/ml)	nd	4.14×10^6	0.12×10^6	0.15×10^6	0.02×10^6	nd	nd
Pasteurella spp. (CFU/ml)	nd	nd	0.38×10^6	1.28×10^6	1.02×10^6	0.18×10^6	0.03×10^6
Pseudomonas mendocina (CFU/ml)	nd	nd	0.56×10^6	1.42×10^6	1.21×10^6	0.28×10^6	0.08×10^6
Total number of fungi (CFU/ml)	1.74×10^5	0.51×10^5	3.48×10^5	1.24×10^5	0.36×10^5	0.14×10^5	0.06×10^5
Sulphate-reducing bacteria (MPN/100 ml)	$2{,}400 \times 10^3$	2.4×10^3	2.4×10^3	1.3×10^3	1.3×10^3	130×10^3	24×10^3
Iron bacteria belonging to the genus *Leptothrix* (MPN/100 ml)	<50	<50	230	230	230	230	230
Iron bacteria belonging to the genus *Siderocapsa* (MPN/100 ml)	2.4×10^5	24×10^5	240×10^5	240×10^5	24×10^5	24×10^5	2.4×10^5

Note: nd—not determined.

Table 3
Number of bacteria and fungi at the water–fuel interphase

Determination	Duration of the studies (d)						
	0	7	14	21	28	35	42
Total number of bacteria, including	2.72×10^6	1.92×10^6	1.34×10^6	0.42×10^6	4.42×10^6	0.42×10^6	3.42×10^6
Sphingobacterium multivorum (CFU/ml)	nd	nd	0.86×10^6	0.32×10^6	3.32×10^6	0.28×10^6	3.15×10^6
Total number of fungi (CFU/ml)	1.82×10^5	1.42×10^5	0.79×10^5	0.21×10^5	0.58×10^5	0.10×10^5	0.21×10^5
Sulphate-reducing bacteria (MPN/100 ml)	$2{,}400 \times 10^3$	nd	nd	nd	nd	130×10^3	24×10^3
Iron bacteria belonging to the genus *Leptothrix* (MPN/100 ml)	<50	<50	<50	<50	<50	130	130
Iron bacteria belonging to the genus *Siderocapsa* (MPN/100 ml)	2.4×10^5	2.4×10^5	24×10^5	240×10^5	24×10^5	2.4×10^5	24×10^5

Note: nd—not determined.

Table 4
Number of bacteria and fungi on St3S steel discs placed in the water

Determination	Duration of the studies (d)						
	0	7	14	21	28	35	42
Total number of bacteria, including	nd	0.04×10^6	0.12×10^6	1.38×10^6	2.52×10^6	3.42×10^6	3.58×10^6
Pasteurella spp. (CFU/cm^2)	nd	nd	0.04×10^6	0.58×10^6	1.32×10^6	1.58×10^6	1.56×10^6
Pseudomonas mendocina (CFU/cm^2)	nd	nd	0.05×10^6	0.52×10^6	1.80×10^6	1.54×10^6	1.52×10^6
Total number of fungi (CFU/cm^2)	nd	0.06×10^5	0.14×10^5	0.62×10^5	0.91×10^5	1.28×10^5	1.18×10^5
Sulphate-reducing bacteria (MPN/100 cm^2)	nd	2.4×10^3	2.4×10^3	24×10^3	24×10^3	240×10^3	240×10^3
Iron bacteria belonging to the genus *Leptothrix* (MPN/100 cm^2)	nd	<50	<50	<50	<50	130	130
Iron bacteria belonging to the genus *Siderocapsa* (MPN/100 cm^2)	nd	0.24×10^5	0.24×10^5	2.4×10^5	2.4×10^5	2.4×10^5	24×10^5

Note: nd—not determined.

Table 5
Number of bacteria and fungi growing on St3S steel samples placed at the water–fuel interphase

Determination	Duration of the studies (d)						
	0	7	14	21	28	35	42
Total number of bacteria, including	nd	0.14×10^6	0.82×10^6	2.48×10^6	3.62×10^6	4.38×10^6	572×10^6
Sphingobacterium multivorum (CFU/cm^2)	nd	nd	0.64×10^6	2.38×10^6	3.18×10^6	4.02×10^6	5.08×10^6
Total number of fungi (CFU/cm^2)	nd	0.07×10^5	0.28×10^5	0.92×10^5	1.74×10^5	2.08×10^5	2.18×10^5
Sulphate-reducing bacteria (MPN/100 cm^2)	nd	0.24×10^3	2.4×10^3	24×10^3	240×10^3	240×10^3	$2{,}400 \times 10^3$
Iron bacteria belonging to the genus *Leptothrix* (MPN/100 cm^2)	nd	<50	<50	<50	<50	130	130
Iron bacteria belonging to the genus *Siderocapsa* (MPN/100 cm^2)	nd	0.24×10^5	2.4×10^5	24×10^5	24×10^5	240×10^5	240×10^5

Table 6
Results of gravimetric studies of St3S steel samples exposed to the aqueous phase

Mean loss of mass (g)	Time of exposure (d)	V_m rate (g/m^2 d)	V_p rate (mm/y)
0.01085	7	0.32	0.014
0.021	14	0.31	0.014
0.0296	21	0.29	0.013
0.0303	28	0.22	0.010
0.0461	42	0.23	0.010
0.076	56	0.28	0.013

Table 7
Results of gravimetric studies of St3S steel samples exposed to the water–fuel interphase

Mean loss of mass (g)	Time of exposure (d)	V_m rate (g/m^2 d)	V_p rate (mm/y)
0.008825	7	2.00	0.093
0.019475	14	2.21	0.102
0.0276	21	2.09	0.097
0.033	28	1.88	0.087
0.0462	35	2.10	0.097
0.0566	42	2.14	0.099

The chemical composition of the corrosion products formed (oxides, hydroxides and iron sulphides) after 47 d indicates considerable loss of metal on the entire surface of the St3S carbon steel disc.

The literature data indicate that it is difficult to compare corrosion weights in different environments. Taseva et al. [13] studied steel coupons in cooling water from a refinery, in which oil contaminations were found; the COD of the water was 45 mg O_2/L. At temperatures changing from 14 to 28˚C, the weight of corrosion was 0.5 mm/y and it was higher than the value obtained in our current study in both the water layer and the water–fuel interphase. The corrosion products were iron sulphides—pyrite and pyrolite, indicating the presence of SRB. In turn, Ilhan-Sungur et al. [14] determined the weight of corrosion of galvanized steel in the water environment in the presence of SRB. The weight was found to decrease over a period of 4–744 h from 76.4 to 1.8 mg/d m^2 d (7,640–180 mg/m^2 d). In this study, the weight of corrosion was not subjected to greater fluctuations and averaged about 3 g/m^2 d in the aqueous phase. The authors studied the products of corrosion using EDS and detected zinc, sulphur, iron, oxygen and phosphorus. They also showed that biocorrosion was caused by SRB, but no correlation between the number of these bacteria and the weight of corrosion was found. SRB requires organic compounds for growth. Xu and

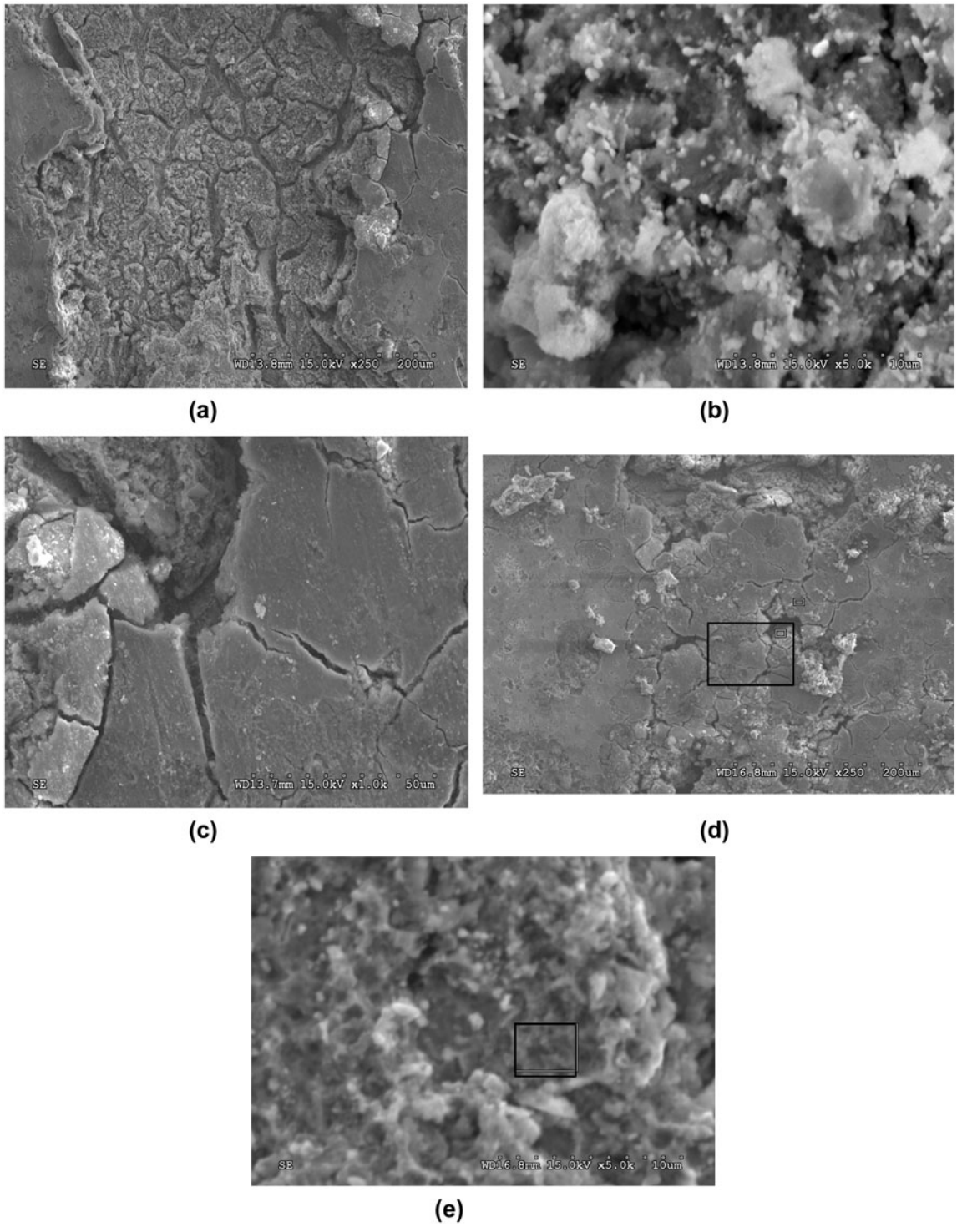

Fig. 1. Image of the damage to the surface of a sample exposed for 7 d at the water–fuel interphase and below the interphase (scanning microscope). Image of the surface of a disc placed in the water–fuel layer (a) visible severe corrosion of the surface; (b) bottom of one of the pits; (c) visible micro-fissures in the material; (d) corroded sample with indicated area on which analysis of the composition of corrosion products was carried out using the EDS method (Fig. 2). Image of the surface of a disc placed below the water–fuel interphase (e) corroded sample with indicated area on which analysis of the composition of corrosion products was carried out using the EDS method (Fig. 3).

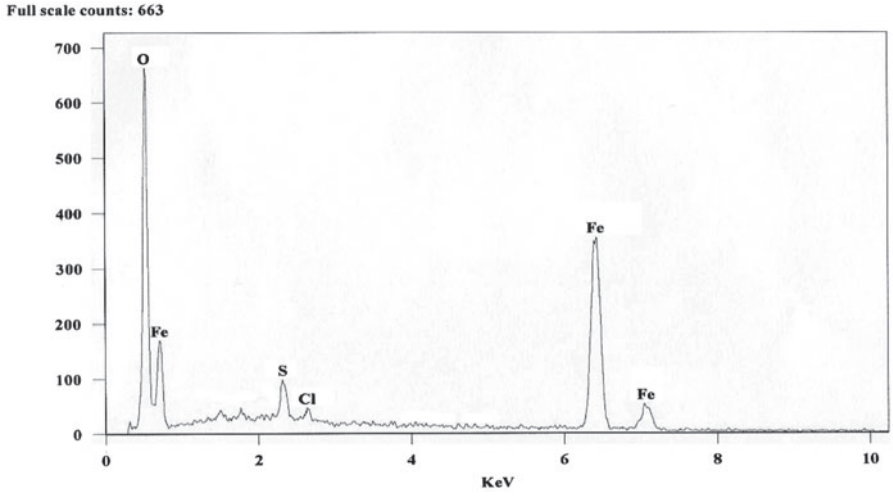

Chemical composition	atomic %	weight%:
O	61,88	32,47
S	2,31	2,43
Cl	0,73	0,84
Fe	35,09	64,26

Fig. 2. The radiation spectrum together with the results of chemical composition of formed corrosion products obtained from the analysed area in Fig. 1(d).

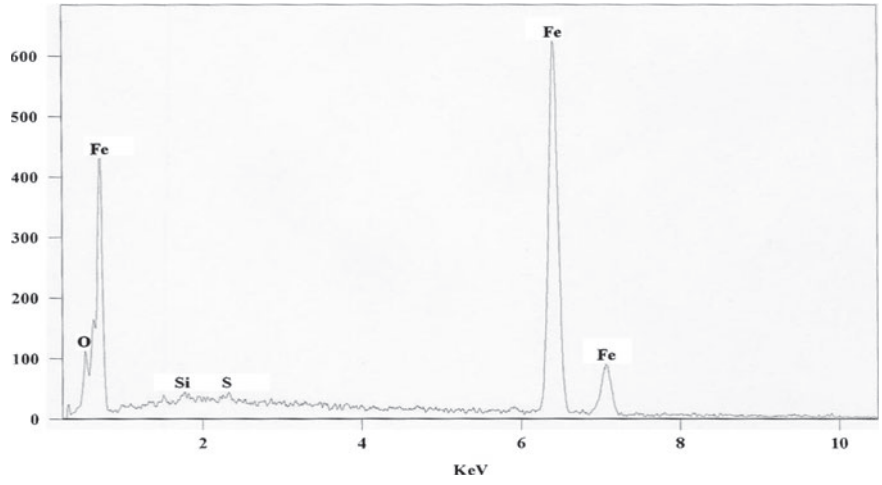

Chemical composition	atomic %	weight%:
O	8,95	2,75
Si	0,66	0,36
S	0,51	0,32
Fe	89,88	96,57

Fig. 3. The radiation spectrum together with the results of chemical composition of formed corrosion products obtained from the analysed area in Fig. 1(e).

Gu [15] showed that the deficiency of carbon sources accelerated the corrosion of carbon steel in the presence of the biofilm formed by *Desulfovibrio vulgaris*. Different concentrations of lactate were used as the carbon source, and the reduction of the content of the compound by 90% significantly lowered the weight of the steel samples. Pits in the discs reached a depth of 10 μm in 7 d.

It is commonly known that the bioenergetic oxidation of iron releases more energy than the oxidation of

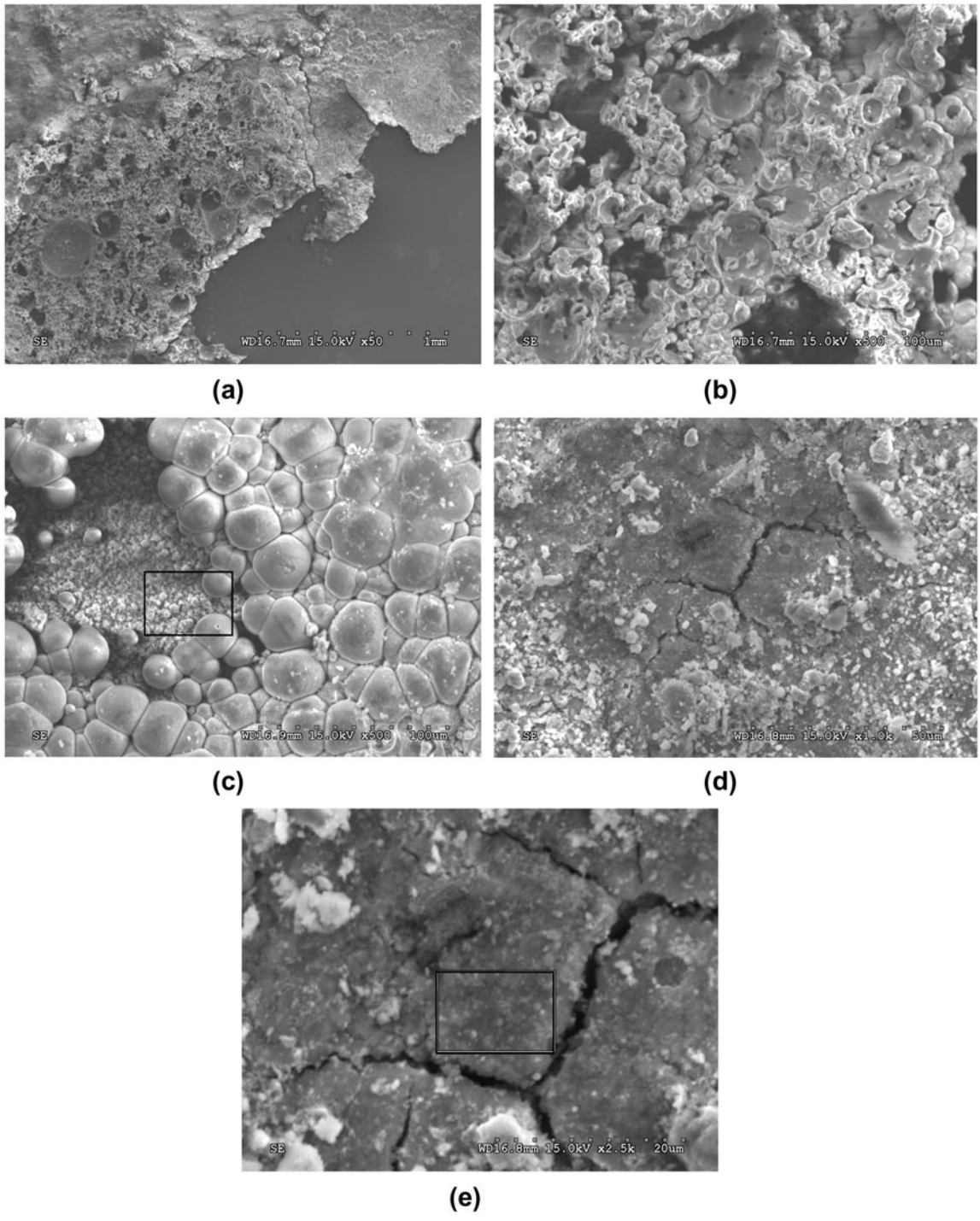

Fig. 4. The image of the damage to the surface of a sample exposed for 47 d at the water–fuel interphase and in the water phase (scanning microscope). The image of the surface of a disc placed in the water–fuel interphase (a) overview of the disc surface; (b) the image of the disc surface placed at the water–fuel interphase; (c) the corroded sample with an indicated area on which the analysis of the composition of corrosion products was carried out using the EDS method (Figs. 5 and 6). The image of the surface of a disc placed in the water layer (d) corrosion deposits on a disc placed below the water–fuel interphase; (e) the corroded sample with an indicated area on which the analysis of the composition of corrosion products was carried out using the EDS method (Fig. 7).

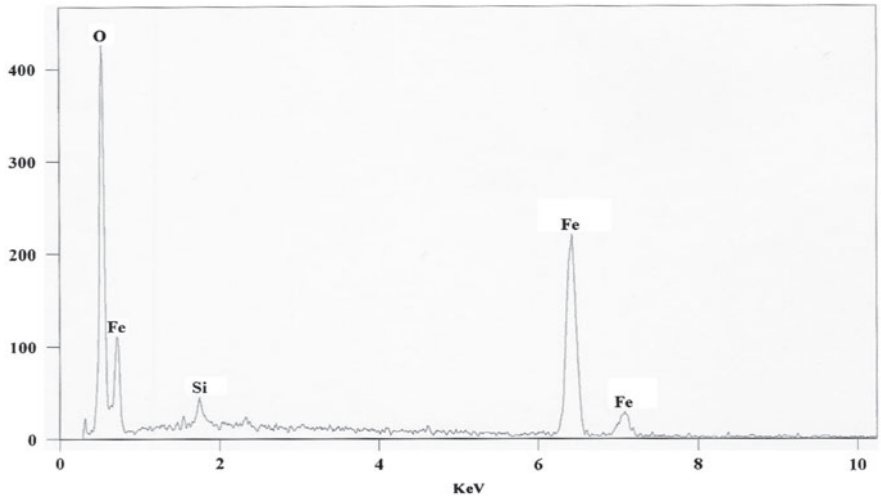

Chemical composition	atomic %	weight%:
O	62.84	33.07
Si	1.44	1.33
Fe	35.71	65.60

Fig. 5. The radiation spectrum together with the results of the chemical composition of formed corrosion products obtained from the analysed area in Fig. 4(c).

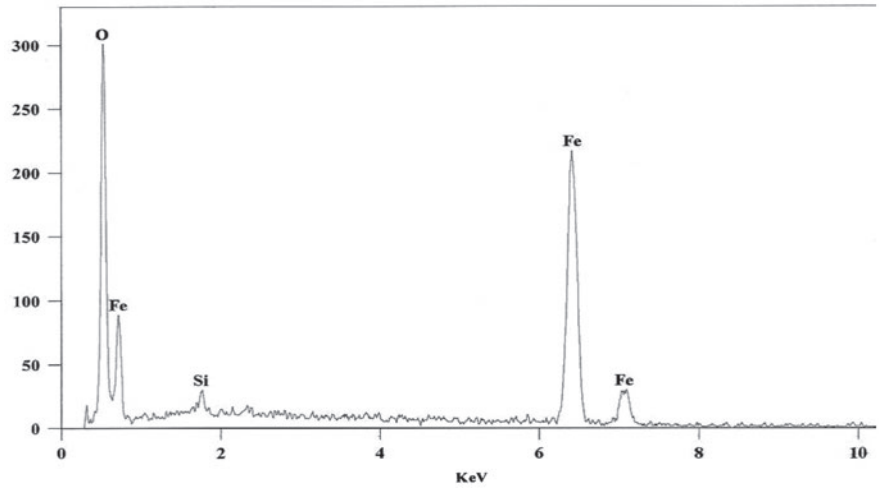

Chemical composition	atomic %	weight%:
O	55.06	26.18
Si	0.92	0.77
Fe	44.02	73.06

Fig. 6. The radiation spectrum together with the results of the chemical composition of formed corrosion products obtained from the analysed area in Fig. 4(c).

lactate, but iron is not an organic source of carbon; hence, "starvation" conditions result in greater aggressiveness of corrosion. The carbon sources for the micro-organisms forming the biofilm in these studies included hydrocarbons, exopolysaccharides and products of cell autolysis. Under these conditions, corrosion processes were observed in spite of a considerable content of organic substances and these were with the participation of SRB. Biocorrosion in aqueous environments has been described in many publications but there is very little data on the destruction of metals in systems containing oil products.

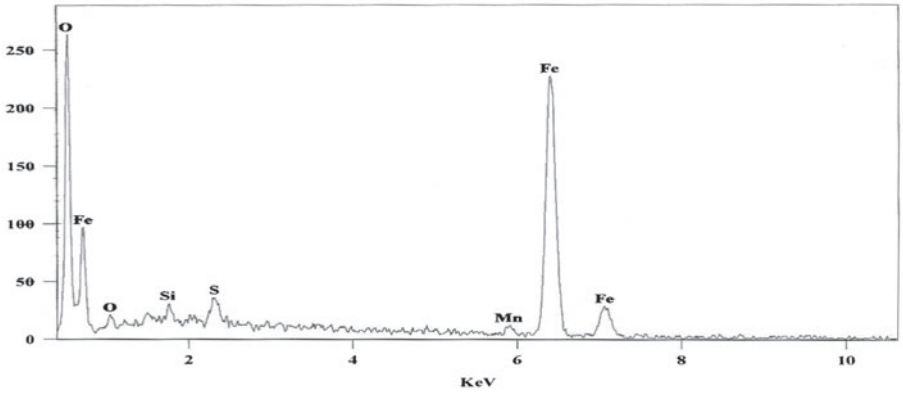

Chemical composition	atomic %	weight%:
O	49.30	22.21
Si	0.88	0.69
S	1.81	1.63
Mn	1.68	2.60
Fe	46.33	72.86

Fig. 7. The radiation spectrum together with the results of the chemical composition of formed corrosion products obtained from the analysed area in Fig. 4(e).

4. Conclusions

Studies on the corrosion of St3S steel in the environment of stored diesel oil revealed that damage to its surface is caused by the development of micro-organisms in the form of a biofilm growing on analysed discs. During the period of one month and a half in which the discs were exposed at the water–fuel interphase, various micro-organisms were found to grow on them, including iron bacteria, SRB and fungi. The weight of corrosion described by the parameters V_p and V_m was over six times higher in the water–fuel interphase than in the water layer. The surface of the discs was characterized by pits up to 130 μm deep (after 47 d) and by the presence of corrosion products compounds of iron with sulphur and oxygen.

The knowledge of the corrosion processes in fuel tanks should be the basis of their proper use and exploitation, and as a result the constant removal of water, cleaning of the tank, mixing of the surface layer of fuel and maintaining the cleanliness of the whole installation.

References

[1] F.M. Bento, Ch.C. Gaylarde, Biodeterioration of stored diesel oil: Studies in Brazil, Int. Biodeterior. Biodegrad. 47 (2001) 107–112.
[2] A. Rajasekar, S. Maruthamuthu, N. Muthukumar, S. Mohanan, P. Subramanian, N. Palaniswamy, Bacterial degradation of naphtha and its influence on corrosion, Corros. Sci. 47 (2005) 257–271.
[3] N.O. San, H. Nazır, G. Dönmez, Microbially influenced corrosion and inhibition of nickel–zinc and nickel–copper coatings by *Pseudomonas aeruginosa*, Corros. Sci. 79 (2014) 177–183.
[4] C. Xu, Y. Zhang, G. Cheng, W. Zhu, Localized corrosion behavior of 316L stainless steel in the presence of sulfate-reducing and iron-oxidizing bacteria, Mater. Sci. Eng., A 443 (2007) 235–241.
[5] I.B. Beech, Corrosion of technical materials in the presence of biofilms—Current understanding and state-of-the art methods of study, Int. Biodeterior. Biodegrad. 53 (2004) 177–183.
[6] L.K. Herrera, H.A. Videla, Role of iron-reducing bacteria in corrosion and protection of carbon steel, Int. Biodeterior. Biodegrad. 63 (2009) 891–895.
[7] Ch. Pillay, J. Lin, Metal corrosion by aerobic bacteria isolated from stimulated corrosion systems: Effects of additional nitrate sources, Int. Biodeterior. Biodegrad. 83 (2013) 158–165.
[8] F. Teng, Y.T. Guan, W.P. Zhu, Effect of biofilm on cast iron pipe corrosion in drinking water distribution system: Corrosion scales characterization and microbial community structure investigation, Corros. Sci. 50 (2008) 2816–2823.
[9] H. Wang, Ch.X. Hu, X. Hu, M. Yang, Effects of disinfectant and biofilm on the corrosion of cast iron pipes in a reclaimed water distribution system, Water Res. 46 (2012) 1070–1078.
[10] E. Huttunen-Saarivirta, M. Honkanen, T. Lepistö, V.-T. Kuokkala, L. Koivisto, C.-G. Berg, Microbiologically influenced corrosion (MIC) in stainless steel heat exchanger, Appl. Surf. Sci. 258 (2012) 6512–6526.
[11] N.O. San, H. Nazır, G. Dönmez, Microbiologically influenced corrosion of NiZn alloy coatings by *Delftia acidovorans* bacterium, Corros. Sci. 64 (2012) 198–203.
[12] Annual Book of ASTM Standard, D 396 Specification of Fuel Oils, vol. 05.01.

[13] V. Taseva, I. Dobrevsky, V. Nenov, N. Dimitrova, B. Bonev, V. Grudeva, A. Novakova, Corrosion processes and control in recirculating cooling water systems in refinery and petrochemical industry, Mater. Corros. 51 (2000) 811–816.
[14] E. Ilhan-Sungur, N. Cansever, A. Cotuk, Microbial corrosion of galvanized steel by a freshwater strain of sulphate reducing bacteria (*Desulfovibrio* sp.), Corros. Sci. 49 (2007) 1097–1109.
[15] D. Xu, T. Gu, Carbon source starvation triggered more aggressive corrosion against carbon steel by the *Desulfovibrio vulgaris* biofilm, Int. Biodeterior. Biodegrad. 91 (2014) 74–81.